

## COMPLEX SPATIAL-TEMPORAL PATTERNS DEVELOPED FROM AN INTERACTION OF FUNCTIONS AND DATA

KOUJI HARADA AND YOSHITERU ISHIDA

Department of Computer Science and Engineering  
Toyohashi University of Technology  
1-1, Hibarigaoka, Tempaku, Toyohashi, Aichi 441-8580, Japan  
{harada; ishida}@cs.tut.ac.jp

Received January 2013; revised May 2013

**ABSTRACT.** *The present study clarifies the complex dynamics produced by removing the formal distinction between data (cell states) and a function (a rule on time evolution of cell states) on two-dimensional cellular automata. While a function usually determines output data, our model incorporates a structure of the function and data determine each other. The immune systems have the similar structure as our model. The introduction of a reciprocal determination process changes the dynamics from unstable simple periodic motions to stable ones. Moreover, to investigate the effect of information instability on the model dynamics, noise (mutation) is imposed on a cell state (data). The mutation enables a transition between dynamical orbits, and creates a meta-attractor that attracts most orbits.*

**Keywords:** Cellular automaton, Immune network, Function, Data, Meta-attractor

**1. Introduction.** The cellular automaton is a computational model driven by simple rules that describes the time evolution of the state of each cell on a defined lattice. Despite its simplicity, it can simulate biological phenomena, as well as physical phenomena such as snow crystal growth and turbulence [1]. A typical cellular automaton is the very popular “game of life”, invented by Conway [2], so-called because it simulates various growth patterns of living systems. In the game of life, the state of a cell at the next time step is determined by the total number of active cells in its neighborhood. Future states evolve by the previous states via a time-invariant rule, which acts forwardly but not inversely. This behavior reflects a formal difference between rule (i.e., function) and states (i.e., data). Most cellular automata are modeled so that rules and data remain completely distinct.

Meanwhile, in the present study, complex dynamics emerge from the mixing of functions and data. This study is motivated by several systems in which functions and data cannot be discriminated. For example, in the immune system, body states such as inflammation (which constitute data) select and activate lymphocytes (functions). The function outputs update the body state (e.g., down regulation of inflammation), as shown in Figure 1. Because it lacks a formal distinction between data and function, the immune system can self-monitor [3,4].

Similarly, Jerne removed idiotype network theory, a new immunological theory in which the antibody (recognizer, equivalent to the function) is indistinguishable from an antigen (recognized entity, equivalent to the data) [5]. This theory underlies an important immunological view called “self-assertion”, which emphasizes a circular causality rather than a linear one [6,7].

The barrier between a function and dummy arguments (data) can be eliminated by the  $\lambda$  calculation, implemented in the Lisp computer language [8]. Applying  $\lambda$  calculus to game theory, Masumoto and Ikegami achieved openness of a strategy space [9]. On the

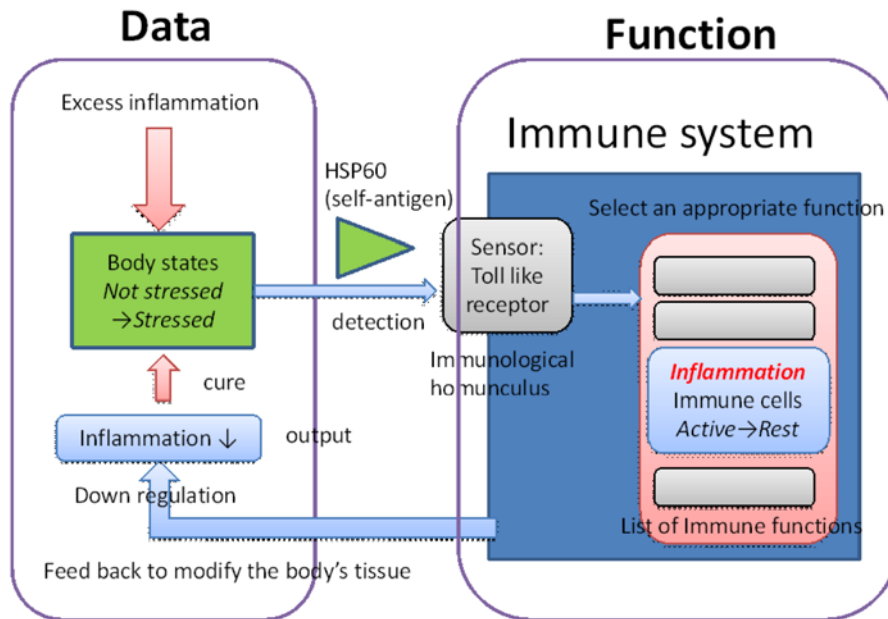


FIGURE 1. Assessment of stress states by the immune system

other hand, Ikegami and Hashimoto proposed a new computational model comprising a set of tapes and a set of Turing machines (Tm). In the model, when a Tm (function) rewrites a tape (data), the tape creates a new Tm, to which it refers its information. Through such mutual interaction, the tape and Tm sets evolve under noise to generate a self-reproducing network called “core network” [10].

Rosen approached the paradox of infinite regression in the metabolic processes of living organisms. Essentially the organism is a self-made machine in which all catalysts must be made, degraded, and replaced within the system by catalysts that are themselves system products, themselves degraded, and replaced by other catalysts ... indefinitely. To circumvent infinite regression, Rosen proposed conceptual models of metabolic network, termed as (M, R) systems [11-13]. In an (M, R) system, catalysts and metabolites are represented as functions as well as input or output data. Rosen stipulated that a metabolite must work as a catalyst and vice versa, as illustrated in Figure 2. In other words, a function equates to data. (M, R) systems were modeled by Letelier et al. in 2006 [14,15].

This study introduces a reciprocal determination process between a rule (function) and cell states (data) on a two-dimensional cellular automaton. A specific process develops complex dynamics, and a meta-attractor emerges under data mutation.

This paper consists of eight sections. The second section proposes a basic two-dimensional cellular automaton driven by a basic rule with no interaction between cell states (data) and an automaton rule (function). This basic model provides a “control” by which to compare the dynamics of a new model allowing data-function interaction. The third section views the cellular automaton as a dynamical system with features such as orbits, periodic orbits, and periodic points. The fourth section presents simple dynamics of the basic model. The novel two-dimensional cellular automaton, which introduces a reciprocal determination process between cell states and an automaton rule, is developed in the fifth section. The sixth section presents all spatial temporal patterns observed in system sizes of  $1 \times 1$ ,  $2 \times 2$  and  $3 \times 3$ , and classifies the emerged dynamics in terms of the periodicity and stability of dynamics. The seventh section focuses on three topics: analogies between our proposed model and a spatial game model besides SIR model, the effect of data mutations on dynamics, and disappearance of a fixed point and appearance

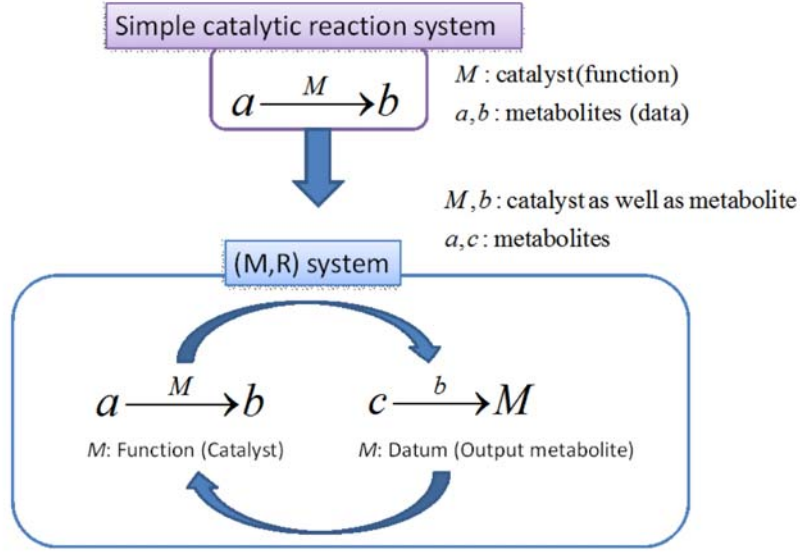


FIGURE 2. Simple catalytic reaction system and an (M, R) system

of a meta-attractor that attracts multiple dynamical orbits. The second topic discusses mutation-induced transitions among unstable and stable orbits, including fixed points, while the last topic demonstrates the Garden of Eden. The eight section concludes the paper.

**2. A Basic Model.** We consider a cellular automaton on a two-dimensional square lattice with sides of length  $N$ . Each cell occupies a site  $(i, j)$  on the lattice, where the indices  $i$  and  $j$  denote the row and column positions, respectively, of the site. The origin is the top-left corner of the lattice. The suffixes  $i$  and  $j$  take an integer value from 0 to  $N - 1$ . We denote a state (0 or 1) of a cell  $(i, j)$  at some discrete time  $r$  by  $A_{i,j}^r$ . The dynamical system of cell state  $A_{i,j}^r$  evolves according to the following linear system:

$$A_{i,j}^{r+1} = F(\vec{b}, \vec{A}_{i,j}^r) \equiv \vec{b} \cdot \vec{A}_{i,j}^r \quad (1)$$

where  $\vec{b}$  is a vector of coefficient parameters, defined as

$$\vec{b} \equiv (b_0, b_1, b_2, b_3, b_4, b_5, b_6, b_7, b_8) \quad (2)$$

with

$$b_i = \begin{cases} 1 & (i = k) \\ 0 & (i \neq k) \end{cases} \quad (3)$$

Here  $k$  is a predetermined parameter.

$\vec{A}_{i,j}^r$  is defined as

$$\vec{A}_{i,j}^r \equiv (A_{i-1,j-1}^r, A_{i-1,j}^r, A_{i-1,j+1}^r, A_{i,j+1}^r, A_{i+1,j+1}^r, A_{i+1,j}^r, A_{i+1,j-1}^r, A_{i,j-1}^r, A_{i,j}^r) \quad (4)$$

As shown in Figure 3, the components of the vector  $\vec{A}_{i,j}^r$  are ordered in a clockwise fashion from the upper-left of site  $(i, j)$ . All cells change their states simultaneously under the local rule Equation (1). Periodic boundary conditions are imposed at the boundary of the two-dimensional lattice. To implement the rule at the edge cells, the lattice space is extended by one line, regarding the lattice as a torus.

As shown in Figure 4, when  $N = 1$  or  $N = 2$ , the left and right lattice spaces are the original and the extended boundary sites, respectively.

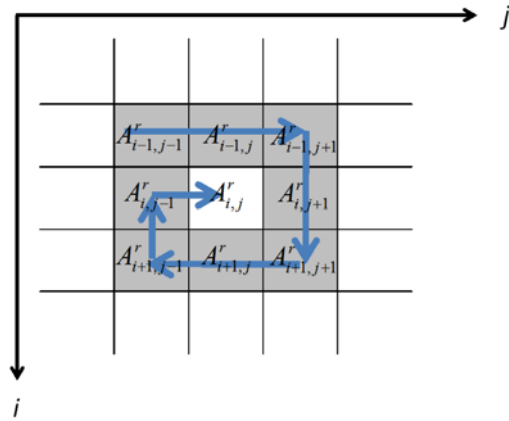


FIGURE 3. Neighborhood of a cell positioned at  $(i, j)$  in state  $A_{i,j}^r$  ( $r$  denotes the time step)

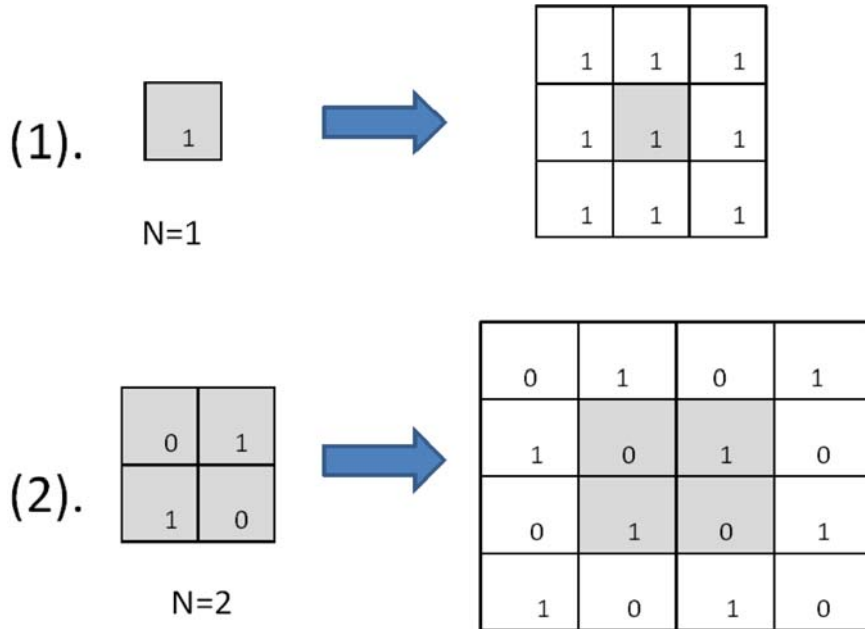


FIGURE 4. Periodic boundary conditions. The left and right lattice spaces are the original and its extended version. (1)  $N = 1$  and (2)  $N = 2$ .

**3. Definition of the Dynamical Orbit.** To implement the cellular automata, we define a map  $G$  that transforms a spatial bit configuration pattern  $P$  into  $P'$  [16] (more precisely, define  $P : N_0^2 \rightarrow \{0, 1\}$ ,  $P \in \{0, 1\}^{N_0^2}$ ). In the basic model,  $G$  is formally constructed by the local rule Equation (1), whereas in the mutual determination model proposed in Section 5,  $G$  is evolved in time according to Equation (8). Applying the map  $G$  repeatedly to an initial pattern  $P^0$ , we obtain a time series of the spatial pattern  $P^0 \rightarrow P^1 (= GP^0) \rightarrow P^2 (= GP^1) \rightarrow \dots$ . Then a set  $\{P^0, P^1, P^2, \dots, P^r, \dots\}$  is called an *orbit*. When an orbit  $\{P^k, P^{k+1}, P^{k+2}, \dots, P^{k+n-1}\}$  satisfies  $P^k = P^{k+n}$ , it is named a *period- $n$  orbit*, and each  $P^i$  ( $i = k, \dots, k + n - 1$ ) is called a *periodic point*. A set of periodic points of a period- $n$  orbit  $O$  is denoted as  $U(O)$ . Other important definitions are listed below.

- The basin  $B(P^i)$  of a periodic point  $P^i \in U(O)$  is a set of spatial patterns  $\{P \mid \exists m > 0 : P^i = G^m P \wedge P \notin U(O)\}$ .
- The basin  $B(O)$  of a period- $n$  orbit  $O$  is defined as  $\bigcup_{i=1}^n B(P^i)$ .

- When  $B(O) \neq \emptyset$ , a period- $n$  orbit  $O$  is “stable”; otherwise it is “unstable”.

The size of the basin  $B(O)$  is defined as  $|B(O)|$ .

**4. Simple Dynamics of the Basic Model.** This section presents the dynamics of the basic model. Assuming periodic boundary of the two-dimensional lattice, a time evolution of spatial-temporal pattern of cell states is easily imagined from the definition of the model. Only periodic motions in one direction, those determined by the vector  $\vec{b}$ , are observed. For example, when  $k = 1$ , Equation (1) becomes  $A_{i,j}^{r+1} = \vec{b} \cdot \vec{A}_{i,j}^r = A_{i-1,j}^r$ , and any spatial-temporal pattern moves downward. If  $k = 3$ , the pattern moves leftward. The periods  $T$  are divisors of  $N$ , for example, when  $N = 4$ ,  $T = 1, 2$  and  $4$  (Figure 5). From the definition of a stable periodic orbit, any periodic orbit observed in the basic model is unstable.

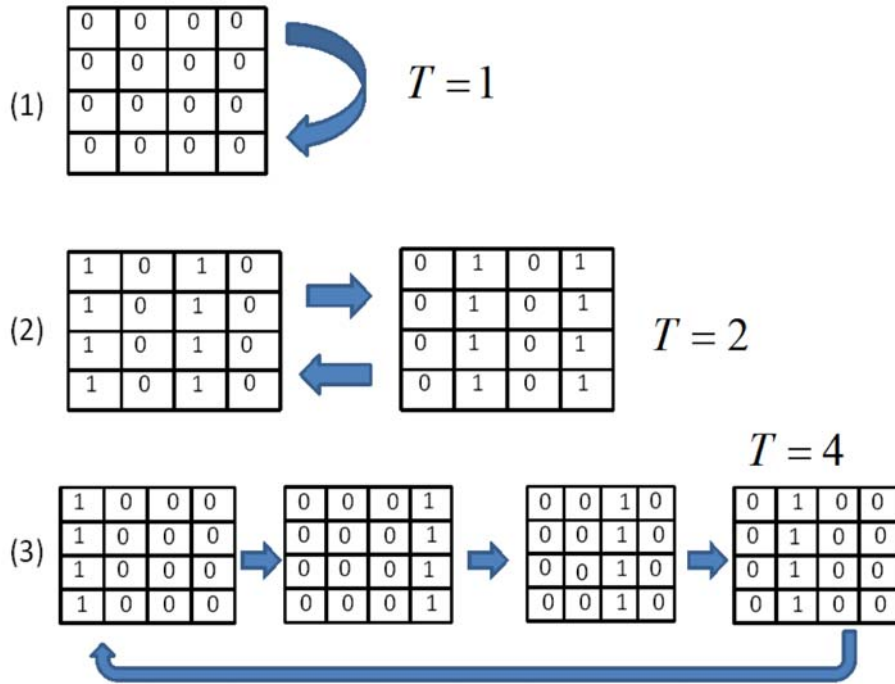


FIGURE 5. Periodic spatial-temporal patterns for  $N = 4$  and  $k = 3$ . (1) Period  $T = 1$ , (2)  $T = 2$  and (3)  $T = 4$ .

**5. A Mutual Determination Model.** This section introduces a reciprocal determination process between the data (cell state) and function (an automaton rule) that updates the parameter  $\vec{b}$  (function selector) through the temporal evolution of the state vector  $\vec{A}_{i,j}^r$ . We define a function  $g(\vec{A}_{i,j}^r)$  as the sum of all cell states in the Moore neighborhood of cell  $(i, j)$ :

$$g(\vec{A}_{i,j}^r) = \sum_{i'=i-1}^{i+1} \sum_{j'=j-1}^{j+1} A_{i',j'}^r - A_{i,j}^r \tag{5}$$

The parameter  $k$  in Equation (3) is dynamically updated with  $g(\vec{A}_{i,j}^r)$  as follows:

$$k^r = g(\vec{A}_{i,j}^r) \tag{6}$$

$$b_i^r = \begin{cases} 1 & (i = k^r) \\ 0 & (i \neq k^r) \end{cases} \tag{7}$$

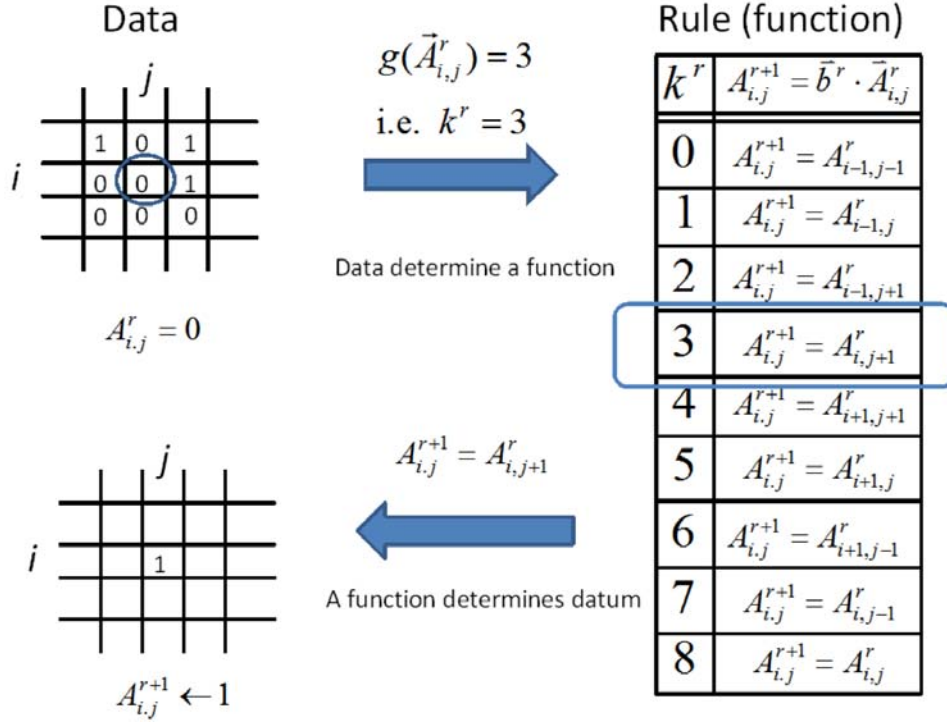


FIGURE 6. Reciprocal determination between data and function

Equation (1) then becomes

$$A_{i,j}^{r+1} = F(\vec{b}^r, \vec{A}_{i,j}^r) \equiv \vec{b}^r \cdot \vec{A}_{i,j}^r. \quad (8)$$

Governed by Equation (8), all cells simultaneously change their states. This model realizes a reciprocal determination between data and function, as shown in Figure 6.

**6. Complex Dynamics of the Mutual Determination Model.** Here we examine all spatial bit patterns observed in systems of size  $(N \times N)$   $1 \times 1$ ,  $2 \times 2$  and  $3 \times 3$ . The emerged dynamics are classified in terms of the periodicity and stability of orbits.

6.1.  $N = 1$ . When  $A_{0,0}^0 = 0$ ,  $k$  is also zero, and  $A_{0,0}^1 = \vec{b}_0 \cdot \vec{A}_{0,0}^0 = A_{0,0}^0 = 0$ . Similarly,

$$\forall t \geq 0, \quad A_{0,0}^t = 0 \quad (9)$$

Equation (9) states that the orbit  $\{0\}$  is a fixed point. The orbit  $\{1\}$  is also a fixed point. Both of these fixed points are unstable.

6.2.  $N = 2$ . The dynamics of the model within a  $2 \times 2$  grid are displayed in Figure 7. The fixed points are A, B, G and H. Especially, the fixed points G and H each attract two spatial bit patterns and are hence “stable”. By contrast, as mentioned in Section 4, the basic model forms no stable orbits. Clearly, the dynamics are stabilized via interactions between the data and the function. On the other hand, dynamics C, D, E and F generate unstable period-2 orbits.

6.3.  $N = 3$ . In this case, the total number of possible spatial bit patterns is 512 ( $= 2^9$ ). Exhaustive analysis revealed that 46 dynamics are possible in this system, most of which are dynamically “stable”, implying the presence of multi-attractors. Among these dynamics, four periodicity classes were identified: period-1 (fixed point), period-3, period-6 and period-9. Spatial bit patterns are encoded in decimal form (Figure 8) so that spatial bit patterns are simply represented as a decimal number.

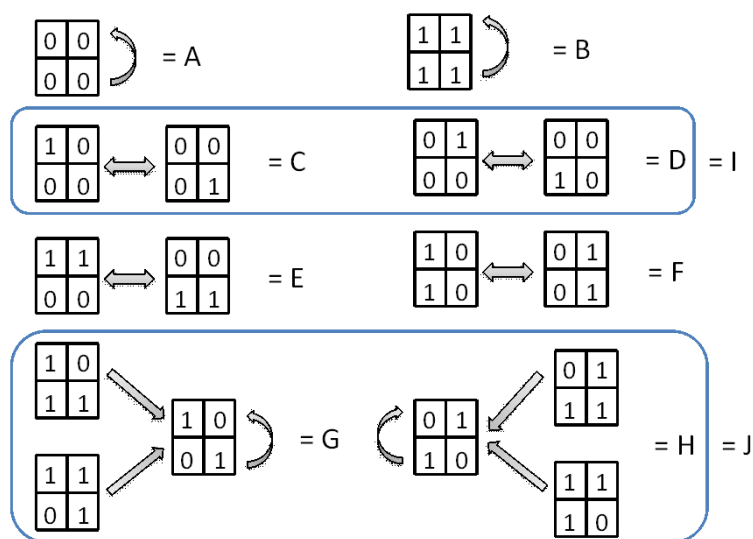


FIGURE 7. Complete dynamics of a data-function interaction model in a  $2 \times 2$  system

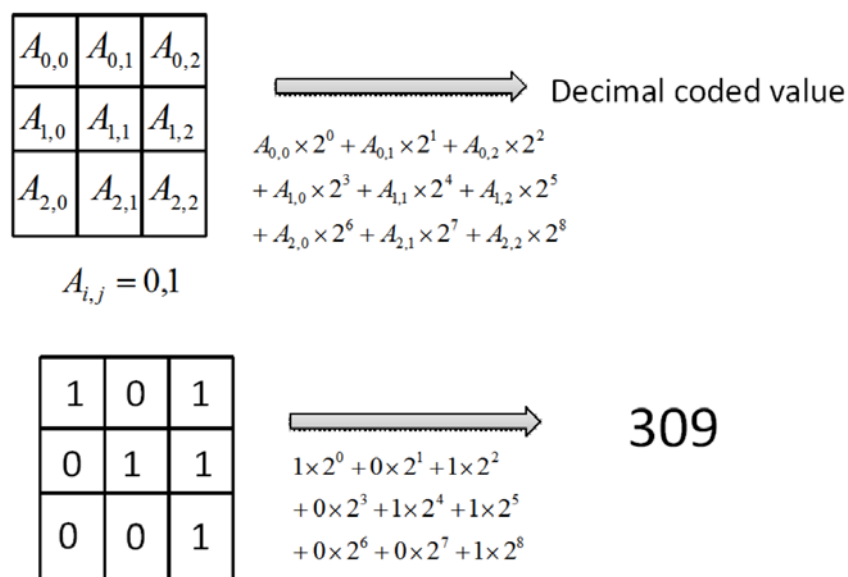


FIGURE 8. Decimal encoding of a  $3 \times 3$  spatial bit pattern

6.3.1. *Fixed-point dynamics.* The above system possesses two stable fixed points (0 and 511; Figure 9). At one of these points, all cells in the pattern equal 1; at the other point, they are 0. The stable fixed points and basins are shown in Figure 9. The basin size of each point is 3.

6.3.2. *Period-3 dynamics.* Figures 10 and 11 illustrate the diverse basin structures and sizes of period-3 orbits. Note that all the observed basins are symmetrically structured.

We now focus on a stable period-3 orbit of extremely broad basin size (Figure 11). Because another stable period-3 orbit exists with the same basin structure, the total basin size of the two attractors is 108. If the system begins with a randomly selected initial configuration, one of the two stable orbits appears with a comparatively high probability  $((54 + 3) \times 2) / 512 \approx 0.22$ . On the other hand, for each transition path in Figure 11, the



FIGURE 9. Fixed-point attractors of basin size 3. Numbers represent the decimal encoding of the spatial bit patterns.

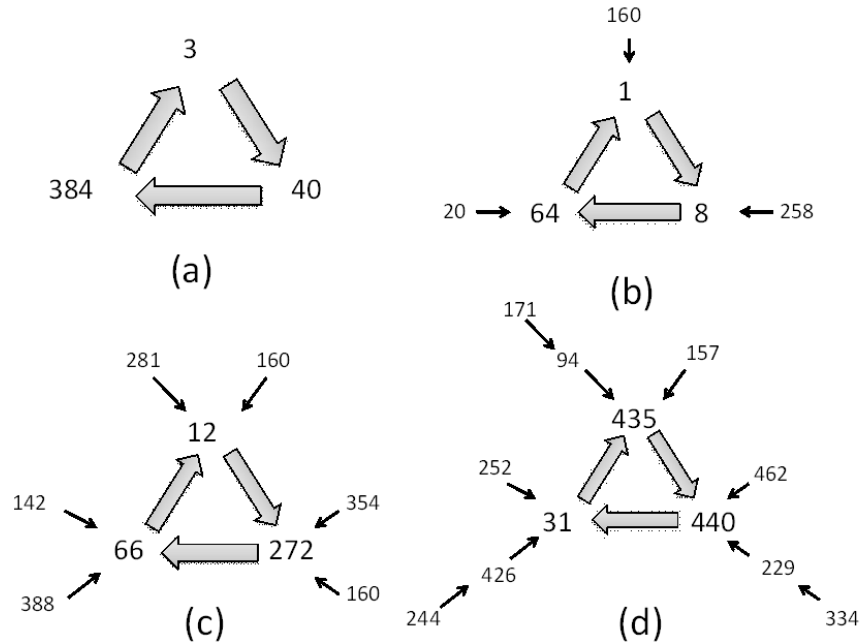


FIGURE 10. Typical forms of period-3 dynamics. Basin sizes are (a) 0, (b) 3, (c) 6 and (d) 9.

periodic point is reached in five steps, while fewer steps are required to reach for other stable period-3 orbits.

6.3.3. *Period-6 dynamics.* A single period-6 orbit is observed (84 → 350 → 266 → 427 → 161 → 245 in decimal form). Because its basin size is zero, this orbit is unstable. The lack of a basin implies that the probability of this orbit emerging from a random initial configuration is rather low, and probably explains the rarity of period-6 orbits.

6.3.4. *Period-9 dynamics.* The longest period observed in the present model is nine. Six period-9 orbits exist in the system, classifiable into two types depending on basin size (Figure 12). Three of the six stable period-9 orbits belong to each class. Period-9 orbits are found when the system begins with a random initial configuration of  $0.32 \left( \frac{(15+9) \times 3 + (21+9) \times 3}{512} \approx 0.32 \right)$ .

6.3.5. *Dominant dynamics.* The results of Sections 6.3.2 and 6.3.4 reveal that stable orbits of period-9 and period-3 (with basin size 54) emerge comparatively often (with probability  $0.32 + 0.22 = 0.54$ ). It follows that these 8 stable orbits (six period-9 orbits and two period-3 orbits of basin size 54) dominate among the 46 dynamical orbits. Such dominant dynamics are not observed in the basic model.



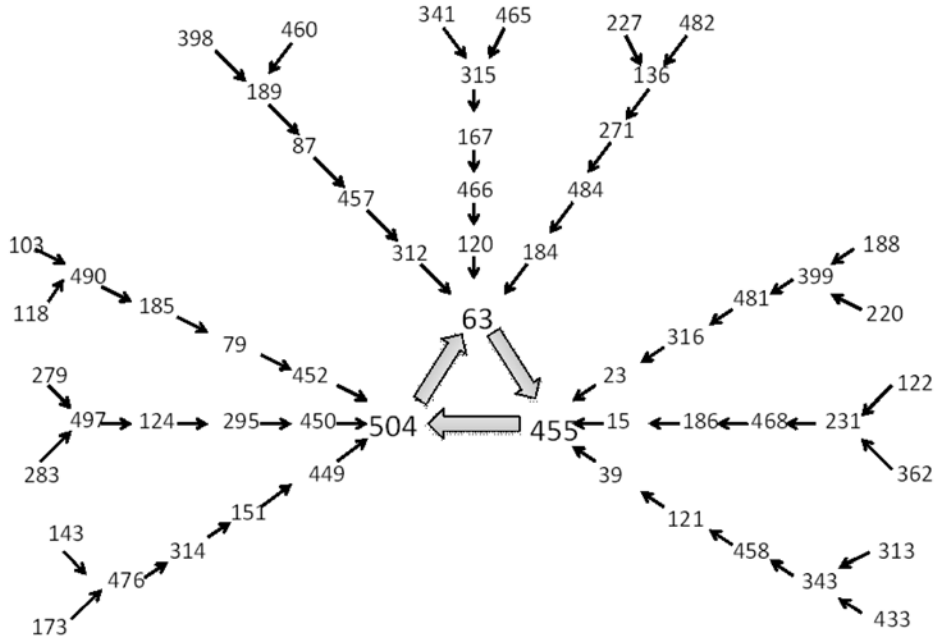


FIGURE 11. An example of period-3 dynamics with a huge basin of size 54

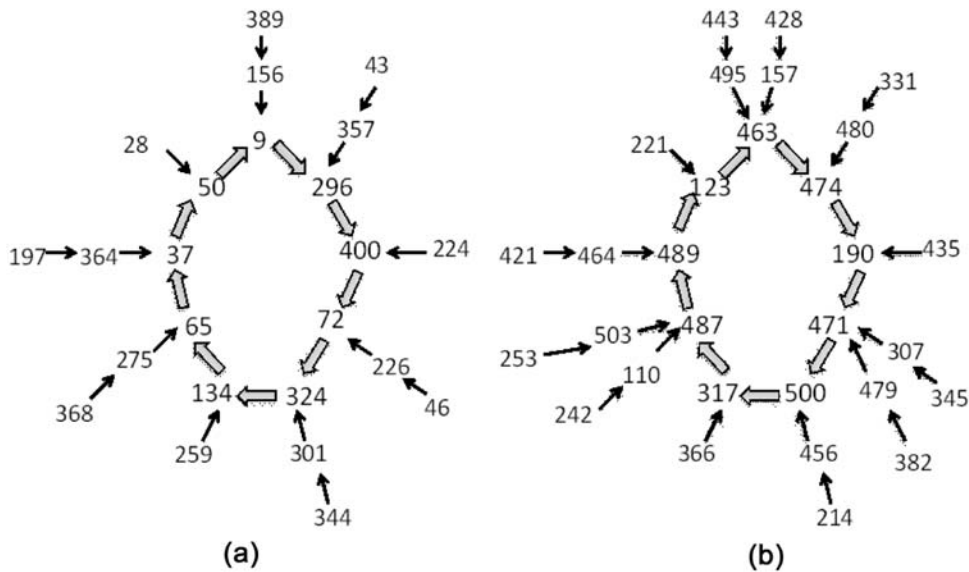


FIGURE 12. Typical forms of period-9 dynamics. Orbits are classified into two classes depending on the basin size: (a) basin size 15 and (b) basin size 21.

## 7. Discussions.

**7.1. Analogy to a spatial game.** Our proposed model is a particular type of spatial game system. In the common spatial game [17], a player plays with each of its neighborhood players and adopts the move of the highest scoring player in the next round. We now demonstrate how our proposed model is related to the common spatial game model. Let cell state  $A_{i,j}^r$  represent the move of a player occupying site  $(i, j)$  at a given time  $r$ ; that is, a player's move is 0 or 1. When the player at site  $(i, j)$  plays with each player in its Moore neighborhood, the highest scoring player is determined by the function  $g(\vec{A}_{i,j}^r)$ .

Specifically, when  $g = k^r$ , our model allows the highest scoring player to occupy the  $k^r$ -th site (clockwise from the top-left of site  $(i, j)$ ). Then, determining  $A_{i,j}^{r+1}$  by Equation (8) is equivalent to the central player copying the move of the highest scoring neighboring player in the next round (known as the copy strategy in common spatial games).

Which winning strategies should a player and its neighbors adopt by the rules of our model? The player can win if all of its neighborhood players simultaneously choose move 1, yielding  $g = 8$ .

In our model, if all players uniformly move 0 or 1, an unstable state results. If any one player takes an opposite move in the uniform state, the system can never return to its original state.

**7.2. Analogy to SIR model.** The mutual determination model is also similar with SIR model without the recovery process on a square lattice. SIR model is a simple model for many contagious diseases with recovery process. The spatial versions of SIR models are studied extensively in several fields [18,19]. Homologizing these models, “1” and “0” states of a cell in the mutual determination model are corresponding to the “susceptible” (S) and the “infected” (I) state of an individual, respectively. In SIR model, a susceptible person on the target site is easier to become infected as more infected individuals are in his neighborhood, while in mutual determination model, the “1” state of the target cell is easier to become “0” state as more cells with “0” state are in its neighborhood. The two fixed points: 0 and 511 in Figure 9 respectively represent the situations that an infection spreads among all individuals on the square lattice and that they are uninfected.

**7.3. Noise on data.** This subsection discusses the effect of information instability on the dynamics of a  $2 \times 2$  system. Noise (mutation) is imposed on a spatial bit pattern (data) corresponding to a fixed point or periodic points. The mutation is implemented by flipping a bit datum of a cell in the spatial pattern. We consider mutations as rare events; that is, a mutation never occurs twice in a row and more than one mutation cannot occur simultaneously. Recall that each of the eight dynamics has been labeled A-H (Figure 7).

The left panel in Figure 13 explains that when a mutation occurs in each of the four cells in the time-invariant pattern, the fixed point A can transit to period-2 orbits C and D. On the other hand, if a fixed point (or periodic orbits) and a transition between any two orbits are regarded as a node and an edge, respectively (the latter terms are used in graph theory), the left panel of Figure 13 can be reinterpreted as the graph in the right panel.

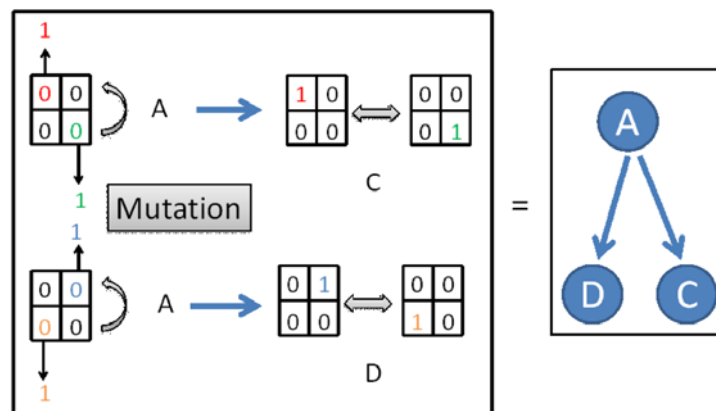


FIGURE 13. Imposing a mutation on a cell state

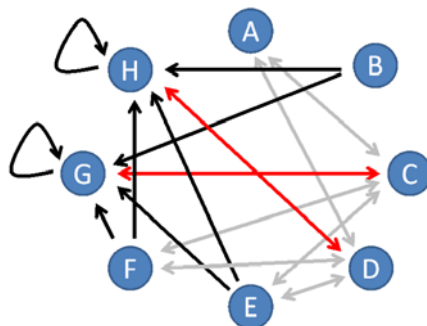


FIGURE 14. Transition paths between periodic orbits, including mutated fixed points. Black edges project toward node G or H, while red edges are bidirectional between nodes G and C or H and D.

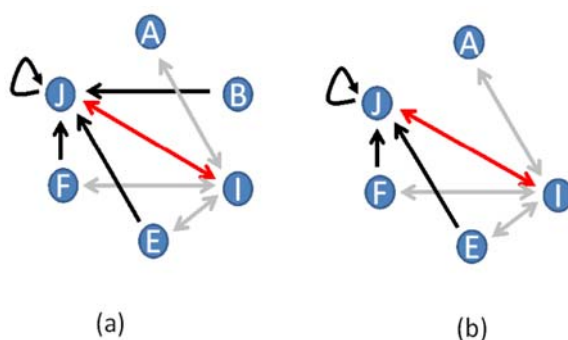


FIGURE 15. (a) This graph simplifies Figure 14 by grouping nodes C and D (G and H) as I (J). Black edges project toward node J, while red edges are bidirectional between nodes I and J. (b) Node B disappears under mutation.

Figure 14 shows all transitions between the eight dynamics from A to H induced by mutations. Three points are worthy of note: (1) The mutation enables a transition between periodic orbits (including fixed points), implying that periodic orbits are no longer time-invariant; (2) A group of nodes appears comparatively stable; (3) Disappearance of a fixed point occurs. Elaborating on the second point, Figure 15(a) shows a graph simplified by grouping nodes C and D (G and H) as I (J). In this graph, five edges are directed toward group J from all nodes (except node A), but a single edge is directed outward from group J. Thus, group J behaves as an almost stable attractor. Group J may be regarded as a meta-attractor because it attracts periodic orbits existing in the absence of mutation. To illustrate the third point, consider node B in Figure 15(a). Edges project from this node but none are directed toward it, implying that mutation never induces a transition toward node B. Thus, node B disappears under mutation. The resulting dynamics are described as a graph in Figure 15(b).

**7.4. Garden of Eden.** The Garden of Eden, named by J. W. Turkey in 1951, is a unique spatial pattern that does not emerge from any preceding spatial patterns. For example, in Figure 10(d), spatial patterns 171, 157, 462, 334, 244 and 252 are Garden of Eden. Essentially, Garden of Eden is a leaf node in a tree whose top node is a periodic point. Interestingly, the basic model precludes a Garden of Eden (because any spatial pattern is a periodic point in a periodic orbit), whereas the mutual determination model permits such nodes. Therefore, Garden of Eden is created by enabling interactions between data and functions.

**8. Conclusion.** This study introduces a reciprocal determination process between data and a function on a two-dimensional cellular automaton. Confusion between data and function enables complex dynamics such as various period orbits, period-3 orbits of huge basin size (54), and Garden of Eden nodes. Furthermore, under data mutation, a meta-attractor emerges, which attracts most orbits despite its imperfect structural stability, while other attractors vanish. These complex dynamics are not observed in the basic model, which maintains a formal boundary between data and function. The mutual interaction between data and function creates a circular relationship (rather than a linear one from input to output) that renders the immune systems self-sustainable [5]. Such self-sustainability is crucial in living systems, and can be properly understood by revealing the diverse dynamics developed by data-function interactions. In future work, we aim to extend self-sustainable dynamics in order to model a self-produced dynamical system and to clarify its characteristics.

**Acknowledgment.** This study was supported by Grant-in-Aid for Scientific Research (C) No. 22500273 of Japan Society for the Promotion of Science (JSPS) from 2010 to 2012. We are grateful for their support.

#### REFERENCES

- [1] J. L. Schiff, *Cellular Automata: A Discrete View of the World*, John Willy & Sons, Inc., 2007.
- [2] G. Martin, Mathematical games, *Sci. Am.*, vol.223, pp.120-123, 1970.
- [3] I. R. Cohen, Real and artificial immune systems: Computing the state of the body, *Nature Reviews Immunology*, pp.569-574, 2007.
- [4] I. R. Cohen, Immune system computation and the immunological homunculus, *Proc. of the 9th MoDELS Conference*, pp.499-512, 2006.
- [5] N. K. Jerne, Towards a network theory of the immune system, *Ann. Immunol.*, vol.125C, no.1-2, pp.373-389, 1974.
- [6] H. Bersini, Self-assertion vs. self-recognition: A tribute to Francisco Varela, *Proc. of the 1st ICARIS Conference*, pp.107-112, 2002.
- [7] H. Bersini, Why the first glass of wine is better than the seventh, *Proc. of the 4th ICARIS Conference*, pp.100-111, 2005.
- [8] J. McCarthy, Recursive functions of symbolic expressions and their computation by machine, Part I, *Comm. ACM*, vol.3, no.4, pp.184-195, 1960.
- [9] G. Masumoto and T. Ikegami, A new formalization of a meta-game using the lambda calculus, *BioSystems*, vol.80, pp.219-231, 2005.
- [10] T. Ikegami and T. Hashimoto, Active mutation in self-reproducing networks of machines and tapes, *Artif. Life*, vol.2, no.3, pp.305-318, 1995.
- [11] R. Rosen, A relational theory of biological systems, *Bull. Math. Biophys.*, vol.20, pp.245-341, 1958.
- [12] R. Rosen, The representation of biological systems from the standpoint of the theory of categories, *Bull. Math. Biophys.*, vol.20, pp.317-341, 1958.
- [13] R. Rosen, A relational theory of biological systems II, *Bull. Math. Biophys.*, vol.21, pp.109-128, 1959.
- [14] J. C. Letelier, G. Marin and J. Mpodozis, Autopoietic and (M, R) systems, *J. of Theor. Biol.*, vol.222, pp.261-272, 2003.
- [15] J. C. Letelier, J. Soto-Andrade, A. F. Guinez, A. Cornish-Bowden and M. L. Cardenas, Organizational invariance and metabolic closure: Analysis in terms of (M, R) systems, *J. Theor. Biol.*, vol.238, no.4, pp.949-961, 2006.
- [16] J. Kari, Theory of cellular automata: A survey, *Theor. Comput. Sci.*, vol.334, pp.3-33, 2005.
- [17] M. A. Nowak and R. M. May, Evolutionary games and spatial chaos, *Nature*, vol.359, pp.826-829, 1992.
- [18] N. C. Grassly and C. Fraser, Mathematical models of infectious disease transmission, *Nat. Rev. Microbiol.*, vol.6, no.6, pp.477-487, 2008.
- [19] N. Boccarda and K. Cheong, Automata network SIR models for the spread of infectious diseases in populations of moving individuals, *J. Phys. A*, vol.25, pp.2447-2461, 1992.